Cascade refrigeration system with inverse Brayton cycle on the cold side

CASCADE REFRIGERATION SYSTEM WITH INVERSE BRAYTON CYCLE ON THE COLD SIDE

Niccolò GIANNETTI [(*)], Adriano MILAZZO[(**)], Andrea ROCCHETTI[(**)], Kiyoshi SAITO[(*)]

[(*)] Waseda University, Department of Applied Mechanics and Aerospace Engineering, 3-4-1 Okubo, Shinjuku-ku, Tokyo 169-8555, Japan

niccolo@aoni.waseda.jp, saitowaseda@gmail.com

Tel/Fax: +81-3-5286-3259 (Japan)

[(**)] University of Florence, Department of Industrial Engineering, Via di Santa Marta 3, Florence, 50139 Italy

adriano.milazzo@unifi.it, andrea.rocchetti@unifi.it

Keywords: Cold-store refrigeration; Cascade system; Inverse Brayton cycle; Performance analysis

ABSTRACT

Low temperature refrigeration of cold stores poses some specific issues: single stage, vapour compression cycles have modest COP at low evaporation temperature; cold evaporator surfaces require de-frosting and a fan for air circulation; a part of the refrigeration load may be delivered at intermediate temperature levels, e.g. for the cold store loading dock.

Cascade system may improve the COP and add flexibility on the temperature levels and working fluids, but the problems related to the cold evaporator surface remain unsolved.

The refrigeration system presented herein features a cascade configuration combining a vapour compression cycle and an inverse Brayton cycle. Both cycles use “natural” fluids, complying with strictest regulations. The top cycle uses Ammonia in order to increase efficiency, while the bottom cycle uses air, which directly circulates in the cold space and hence eliminates the cold heat exchanger. A detailed thermodynamic analysis allows a complete screening of the relevant design parameters for an overall system optimization.

The results show that, notwithstanding the intrinsic gap of efficiency suffered by the Brayton cycle, the proposed system features an acceptable global performance and widens the implementation field of this technology. This system configuration shows a COP 50% higher than the corresponding simple Brayton cycle at temperatures of the refrigerated storage of -50°C.

Nomenclature

A	Cross-section area [m^2]
c_p	Isobaric specific heat [$kJ \cdot kg^{-1}K^{-1}$]
c_v	Isochoric specific heat [$kJ \cdot kg^{-1}K^{-1}$]
COP	Coefficient of performance
G	Mass velocity [$kg \cdot m^{-2}s^{-1}$]
h	Specific enthalpy [$kJ \cdot kg^{-1}$]
J	Humid air specific enthalpy [$kJ \cdot kg^{-1}$]
k	Heat capacity ratio
L	Axial length [m]
$\dot{m}$	Mass flow rate [$kg \cdot s^{-1}$]
P	Absolute pressure [kPa]
Q_f	Cooling load [kW]
r	Latent heat [$kJ \cdot kg^{-1}$]
s	Specific entropy [$kJ \cdot kg^{-1}K^{-1}$]
S	Transfer surface [m^2]
T	Temperature [K]
W	Power [kW]
x	absolute humidity
z	Compressibility factor

Greek symbols

α	Transfer area per unit volume [m^{-1}]
β	Heat transfer coefficient [$W \cdot m^{-2}K^{-1}$]
ε	Thermal effectiveness
η	Efficiency
π	Compression ratio

Subscripts

air	Air
amb	Ambient
aux	Auxiliary fan
B	Inverse Brayton
C	Compressor
cond	Condenser
corr	Accounting for fan and defrost loads
el	Electrical
eva	Evaporator/Cascade heat exchanger
ice	Ice
is	Iso-entropic
LD	Loading dock
max	Maximum
mech	Mechanical
min	Minimum
R	Regenerative heat exchanger
RS	Cold storage
sat	Saturation
sh	Super-heat
T	Expander
v	Water vapour
VC	Vapour compression

1. INTRODUCTION

1.1 Cascade systems

The low storing temperature required by many perishable goods may be efficiently guaranteed by a staged refrigeration system, featuring one or more intermediate temperature levels. This reduces the irreversibilities of the thermodynamic cycle, both on the compression and on the expansion side. Cascade refrigeration systems, when compared to other staged configurations (e.g. double stage with economizer), offer an additional degree of freedom for their optimization, i.e. the choice of a suitable combination of refrigerant fluids, and may offer enhanced performance [1]. Ideally, the refrigerants should be environmentally friendly, non-flammable, non-toxic, and yield the lowest possible initial investment and operative cost.

Several thermodynamic simulations for low temperature refrigeration systems have been reported in the literature. A summary is presented in Table 1. Apparently, NH_3 is the best choice as a fluid for the high temperature cycle (apart from ethanol). CO_2 is often proposed for the low temperature cycle, as it is environmentally safe, non-flammable and non-toxic. However, it has a worsening effect on COP, as shown e.g. by comparing the result of Kilicarslan and Hosoz [2], who used R23, with Lee et al. [3], who used CO_2.

Table 1 – Literature results of simulations for cascade refrigeration systems

Reference	**HT Fluid**	**LT Fluid**	T_{cond}	T_{eva}	**COP**
Aminyavari et al. 2014 [5]	NH_3	CO_2	40	-49	1.5
Nasruddin et al. 2016 [6]	C_3H_8	$C_2H_6 + CO_2$	56	-49	0.79
Di Nicola et al. 2011 [4]	NH_3	C_2H_6	40	-70	0.97
		C_3H_8			1.01
		$C_2H_6 + CO_2$			0.93
		$C_3H_8 + CO_2$			0.87
Gettu, Bansal 2008 [7]	NH_3	CO_2	40	-50	1.43
	Ethanol				1.5
	R404				1.35
Lee et al. 2006 [3]	NH_3	CO_2	30	-55 ÷ -45	1.1 ÷ 1.44
			35		1.01 ÷ 1.31
			40		0.92 ÷ 1.2
Kilicarslan, Hosoz 2010 [2]	NH_3	R23	40	-65 ÷ -45	0.89 ÷ 1.25
	R134				0.77 ÷ 1.08
	R404				0.64 ÷ 0.8
Mosaffa et al. 2016 [8]	NH_3	CO_2	35	-45 ÷ -35	1.17÷1.37

The same result was shown by Di Nicola et al. [4] who compared pure hydrocarbons with mixtures of hydrocarbons and CO_2. Furthermore, CO_2 is unusable at very low temperatures, triple point being at -56.6°C, and requires high operating pressures, increasing the cost of the refrigeration system.

Experimental data on NH_3/CO_2 cascade refrigeration systems have been collected e.g. by Bingmin et al. [1] and by Dopazo and Fernandez-Seara [9]. A comparison between these data and other experimental results on a R134a/CO_2 cascade system (Sanz-Kock et al. [10]) is shown in Fig.1. Once again, NH_3 seems to be a preferable option for the high temperature cycle. Ammonia does pose safety problems, but the refrigeration industry has been using it from the very beginning and has acquired the due experience for managing any possible risk. Ammonia is commonly included among the "natural" refrigerants and is receiving an increasing attention from many global players in the refrigeration area [11]. Furthermore, in a cascade system ammonia may be confined to a restricted part of the plant.

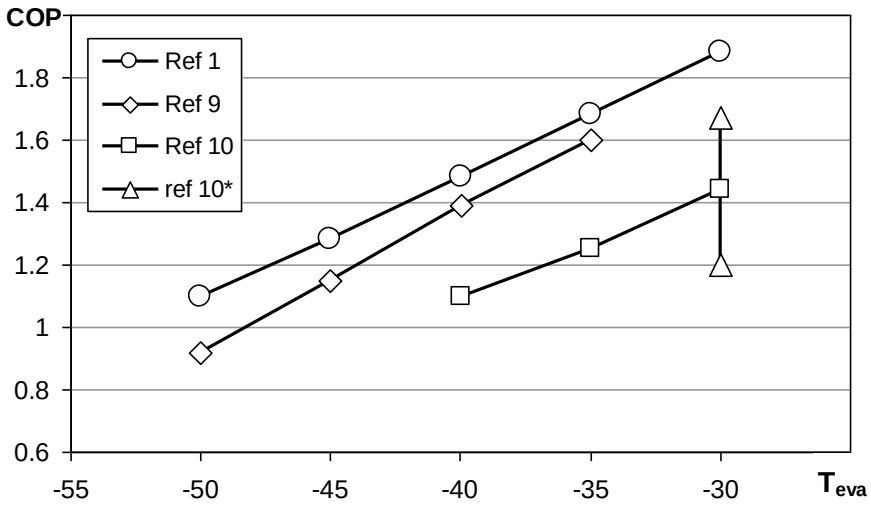

Fig. 1 – Experimental data from the literature on cascade refrigeration systems

Ref. [1]: Bingmin et al.; NH_3/CO_2; T_{cond} =40°C; Ref. [9]: Dopazo, Fernandez-Seara; NH_3/CO_2, T_{cond} =30°C; Ref. [10]: Sanz-Kock et al.; R134a/CO_2; T_{cond} = 40°C; Ref. [10]*: same with T_{cond} = 30-50°C

1.2 Air cycle

A further option for the low-temperature working fluid is air, which may be used in an inverse Brayton cycle. This cycle has been extensively analysed in various configurations and under different evaluation

approaches. Zhang et al. [12] developed an irreversible model and compared the optimal performance of a regenerative cycle with that of a simple Brayton cycle. Chen et al. [13] derived a general expression for the exergetic efficiency of a regenerated air refrigerator, whereas Ust [14] based his cycle optimization on an ecological coefficient of performance (ECOP). Obvious advantages of air as a refrigerant are absolute environmental and operational safety. Air is available everywhere at no cost, which has prompted its use as working fluid in many devices from the early stages of civilization, immediately after water [15]. Not surprisingly, among the first refrigeration systems we find the air machine patented by John Gorrie that dates back to the first half of the 19th century and had a good success until the introduction of synthetic refrigerants [16]. Perishable goods are normally stored in air, so that this same air can be used as working fluid by opening the cycle on the cold side (**high pressure cycle** – Fig. 2a), whence the low temperature heat exchanger is eliminated. Alternatively, we may use the ambient air as working fluid, eliminating the high temperature heat exchanger (**low pressure cycle** – Fig. 2b).

Grazzini and Milazzo [17] have shown that, in both cases, an open cycle yields a significant increase in efficiency, but the low pressure configuration of Fig.2b is somewhat better. On the other hand, the high pressure scheme of Fig. 2a has the major advantage of eliminating the cold heat exchanger which, when operated below 0°C, is prone to frost accumulation.

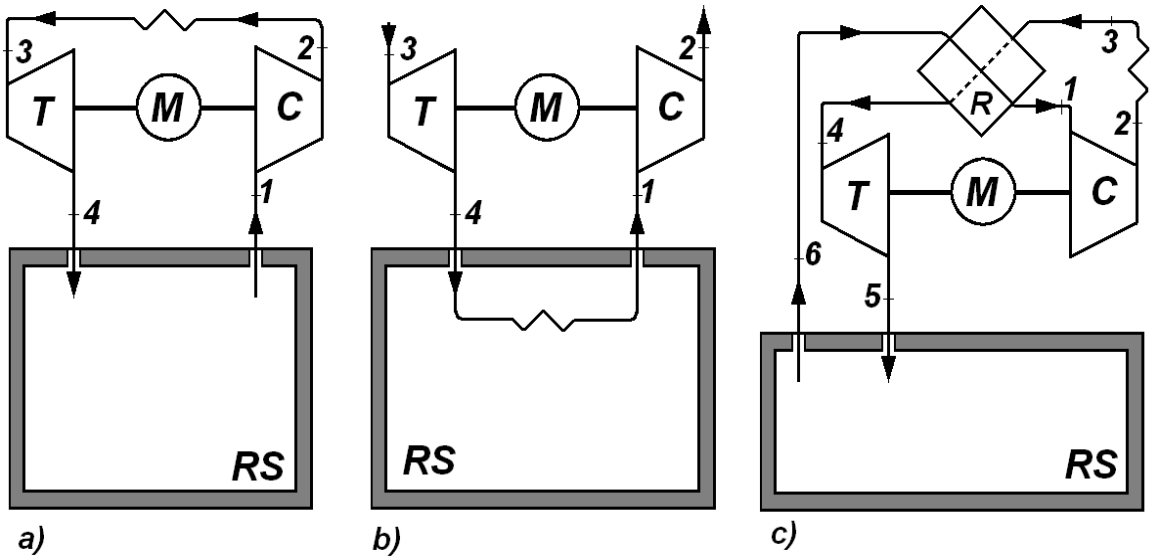

Figure 2. Inverse Brayton cycles; a) high pressure; b) low pressure; c) regenerated

M: electric motor; C: compressor; T: turbine; R: regenerator, RS: refrigerated space.

The inevitable ingestion of the air humidity causes water condensation and eventually icing in the cold sections of the system, but the ice particles are formed within the air stream and, as far as they are small, they move with the air flow, instead of sticking on a cold surface which must be periodically defrosted. The ice particles can be captured, allowing some humidity control.

As far as the residual air velocity at turbine exit is sufficient, even the electric fan that normally circulates the cold air within the cell (and adds a further electric and thermal load) may be eliminated.

The inclusion of a regenerative heat exchanger (Fig. 2c), increases efficiency and reduces the performance gap between the high and low pressure configuration as shown by Giannetti and Milazzo [18]. This component plays a crucial role in the thermodynamic optimization of the whole system, as will be shown later.

A cascade configuration employing an inverse Brayton as the bottom cycle was suggested by Nobrega and Sphaier [19] or Elsayed et al. [20], who used a desiccant top cycle. However, to the authors' knowledge, a cascade of a standard vapour compression cycle and an open inverse Brayton was not discussed in previous literature, and the integration of these two well-established technologies could be useful to overcome some of their downsides for a cold store application. The present proposal may be near to market application and worth of a detailed analysis in terms of design parameters and expected performance. Additionally, the effect of the phase change of the humidity carried from the air stream circulating within the Brayton cycle is accounted for in the present modelling effort. The air expansion is reconstructed as a series of equilibrium states to accurately predict the conditions of the air at the outlet of the expander, which can considerably deviate from the results obtained for an ideal-gas behaviour. An accurate prediction of the outlet stream properties in the cold store is critical for an accurate design and optimization of the specific plant. Moreover, ice separation from the expanding air stream represents a promising alternative to the traditional defrosting process of aero-evaporators used in cold stores and an evaluation of its potential may be useful.

2. SYSTEM ANALYSIS

From a practical point of view, an air cycle refrigeration system may be fairly simple, with compressor and turbine on a single shaft, driven by a high speed electric motor. Magnetic bearings reduce friction and allow

a completely oil-free operation. These concepts are well proven by state-of-the-art centrifugal compressors which are gaining an increasing market share in many refrigeration applications. The avoidance of a closed cycle (which could present fluid leakage) increases reliability. Highly efficient compressor, turbine and heat exchangers are required in order to achieve acceptable COP. The residual efficiency gap with respect to vapour compression plants must be evaluated on a system basis and over a seasonal operating period that includes defrosting cycles.

Regeneration, i.e. internal heat exchange between the warm air on the high-pressure side of the cycle and the cold air on the low-pressure side (Fig 2c), allows to overcome the constraint that links the compression ratio of the simple cycle to the temperature range to be covered.

The approach featuring a high pressure, regenerated cycle with single-stage compression is confirmed by a refrigeration system named "Pascal Air", manufactured in Japan by Mayekawa [21] and a similar system developed by Mitsubishi [22]. Another system, the "AIRS50", featuring a staged compression [23] was developed by Kajima Inc. and later by Earthship Ltd. and reached a pre-commercial stage of development, but is no longer available.

In the case of a food storage facility, a loading/shipping dock is common everywhere and absolutely necessary in humid and warm climates. The benefits of a refrigerated loading dock are [24]:

- The refrigeration load in the low-temperature storage (where the energy demand per unit capacity is higher) is reduced;
- A lower amount of humid air is infiltrated in the low-temperature area, reducing ice formation;
- Refrigerated products held on the dock for loading/shipping maintain their quality;
- Products packaging, equipment and floor areas stay drier, increasing goods quality, system reliability and operators' safety.

The loading dock (*LD*) is normally kept around 5°C. The combined need for a low temperature refrigerated space and intermediate temperature loading dock may be favourably satisfied by a cascade refrigeration concept that has an intermediate heat exchanger between the two cycles.

A hybrid vapour compression / inverse Brayton cascade system may be envisaged as follows (Fig. 3): the top cycle 7-8-9-10 could be any high temperature vapour compression system, featuring a compressor *C*, a condenser *K*, an expansion valve *EV* and two evaporators E_1 and E_2. The first evaporator refrigerates the

loading dock *LD*, while the second couples the vapour compression and the inverse Brayton cycle, cooling down the hot compressed air between points 2 and 3. The regenerator further cools the air flow between points 3 and 4. The expansion brings the air back to ambient pressure and produces the minimum system temperature at point 5. The exhaust air 6 from the refrigerated space *RS* is warmed up in the regenerator before entering the compressor in 1. Auxiliary components (e.g. liquid receiver at condenser exit) and other practical issues (load control, etc.) are not included in this analysis, which is mainly devoted to thermodynamics for a preliminary system design and screening of its potential.

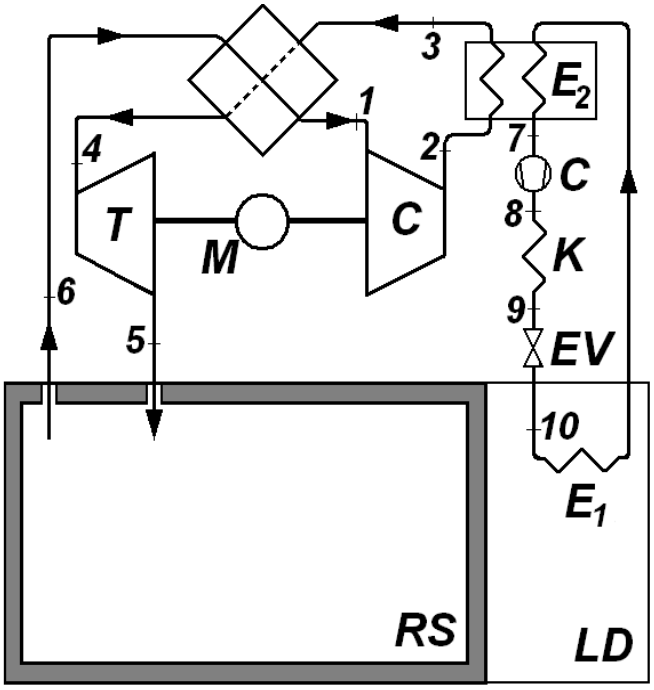

Figure 3. Scheme of the proposed plant

2.1 Thermodynamic modelling

The system efficiency may be expressed by a coefficient of performance defined as:

$$COP = \frac{Q_{f-RS} + Q_{f-LD}}{W_B + W_{VC} + W_{aux}} \quad (1)$$

where Q_f = cooling load [kW], W_B = input power for Brayton cycle [kW], W_{VC} = input power for vapour compression cycle, W_{aux} = auxiliary power input (condenser fan, etc.).

The corresponding thermodynamic cycles are shown on a *Ts* diagram in Fig. 4 for the preliminary design values of the operative parameters listed in Table 2.

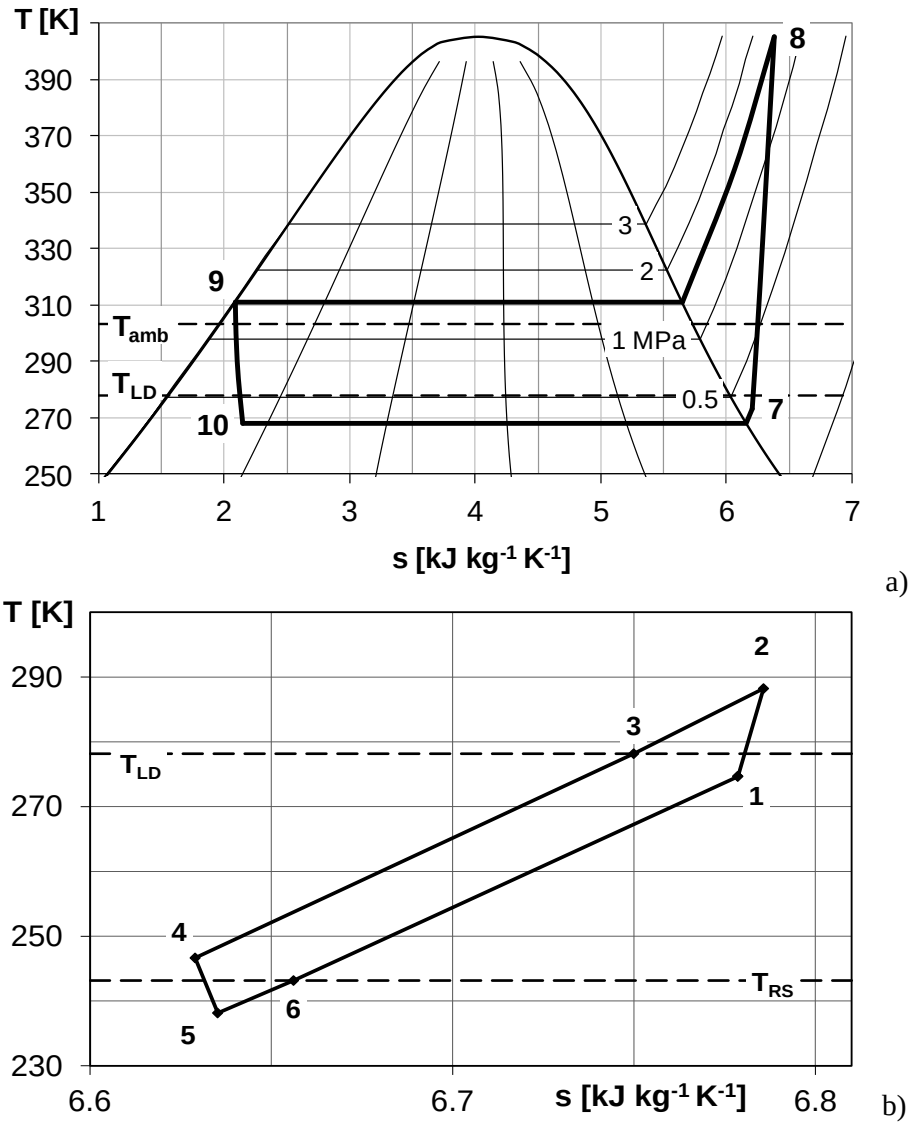

Figure 4. Temperature-entropy diagrams of the top (a) and bottom (b) cycles

Table 2 – Reference system parameters.

Refrigerated store temperature (°C)	T_{RS}	-30
Loading dock temperature (°C)	T_{LD}	5
Ambient temperature	T_{amb}	30
Minimum temperature difference at heat exchangers (°C)	$\Delta T_{eva,min}$	10
Top cycle		
Fluid		NH_3
Evaporation temperature (°C)	T_{10}	-5
Condensation temperature (°C)	T_9	40
Superheating at evaporator (°C)	ΔT_{sh}	5
Subcooling at condenser outlet (°C)	ΔT_{sc}	0
Cooling capacity (kW)	$Q_{f\text{-}VC}$	103
Input power (kW)	W_{VC}	26.5
Fluid temperature at compressor outlet (°C)	T_8	132
Air cycle		
Temperature difference between inlet cold air and store (°C)	$\Delta T_{5\text{-}6}$	10
Specific heat ratio (air)	k	1.4
Regenerative heat exchanger effectiveness	ε_R	0.9
Compression efficiency	η_C	0.85
Expansion efficiency	η_T	0.85
Combined mechanical and electrical efficiencies	$\eta_{mech}\eta_{el}$	0.9

The high temperature cycle is calculated using the selection software available at the compressor manufacturer website (https://www.bitzer.de/websoftware/Calculate.aspx [25]). NH_3 is assumed as the working fluid. The compressor performance and the working cycle are specified according to EN 12900. The selected compressor is an open, reciprocating unit with 6 cylinders, operating at 50 Hz (Bitzer W6FA). The performance of the top cycle is summarized in Fig. 5 for two evaporation temperatures. Note that this temperature is related to the loading dock temperature and hence is not used as a design parameter in this analysis. The conservative value T_{eva} = -5°C (i.e. 10°C temperature difference between evaporation and loading dock temperature) is assumed hereafter. The *Ts* diagram in Fig. 4a is calculated by NIST REFPROP [26] functions.

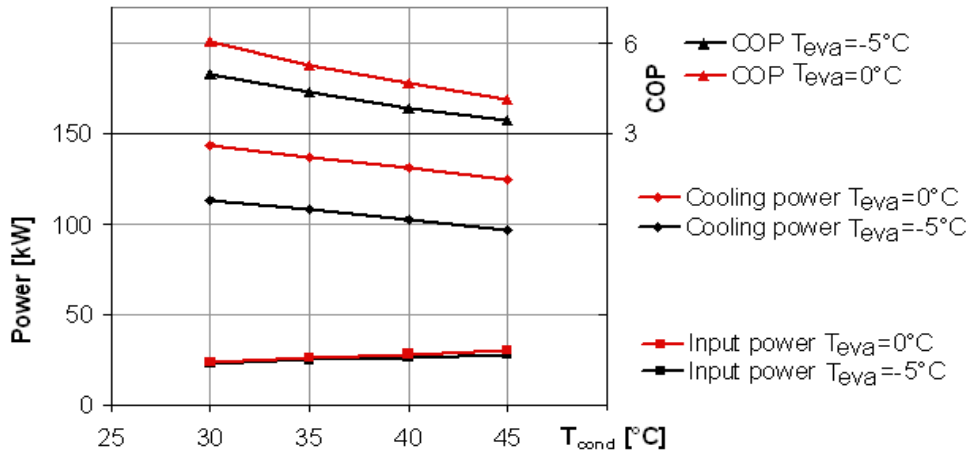

232

233 Fig. 5. High temperature cycle performance

234

235 For the bottom cycle (Fig. 4b), air is modelled as an ideal gas, compressibility factor $z = Pv / RT$
236 being unitary within 2‰ in the relevant pressure and temperature range ($230 < T < 310$ K; $0.1 < P < 0.2$
237 Mpa). Air specific heat ratio $k = c_p / c_v$ is assumed constant in the same range, its variations being of the
238 same order. Air enthalpy and entropy are calculated by NIST REFPROP [26] functions.

239 Air humidity is taken into account, assuming saturation within the refrigerated space. Unfortunately,
240 NIST [26] functions for water are unavailable below 0°C. Therefore, water vapour properties are taken from
241 ASHRAE Fundamentals Handbook [27]. Unless an extremely efficient regenerator is available, absolute
242 humidity remains constant through the cycle, until phase change occurs in the turbine. Ice particles may be
243 captured by suitable filters (NEDO documents [28]) placed at inlet and outlet air ports within the refrigerated
244 space, in order to perform active de-humidification (air introduced in the refrigerated space at point 5 has
245 lower absolute humidity than that drawn at point 6).

246 Losses within compressors and turbine are accounted for by isentropic efficiencies:

247 $$\eta_C = \frac{W_{C-is}}{W_C}; \quad \eta_T = \frac{W_T}{W_{T-is}} \tag{2}$$

248 When the compressor and expander are assembled on a single shaft, the electric motor of the Brayton
249 cycle consumes a power

250 $$W_B = \frac{W_C - W_T}{\eta_{mech}\eta_{el}} \tag{3}$$

The regenerator effectiveness ε_R, neglecting the specific heat variation, is given by:

$$\varepsilon_R = \frac{T_3 - T_4}{T_3 - T_6} = \frac{T_1 - T_6}{T_3 - T_6} \tag{4}$$

Cycle point numbering is specified in Fig. 4.

The regenerator inlet temperatures are $T_6 = T_{RS}$ and T_3, which is fixed by setting a minimum temperature difference between air flow and evaporating fluid temperature T_{10}. The inverse Brayton cycle is hence calculated as follows (cycle points are numbered as in Fig. 2):

$$T_5 = T_{RS} - \Delta T_{5-6};\ \ T_3 = T_{10} + \Delta T_{\min};\ T_4 = T_3 - \varepsilon_R (T_3 - T_6);\ T_1 = T_6 + \varepsilon_R (T_3 - T_6) \tag{5}$$

Temperature T_2 is a function of the compression ratio $\pi = P_2 / P_1$:

$$T_2 = T_1 \left[1 + \frac{1}{\eta_C} \left(\pi^{\frac{k-1}{k}} - 1 \right) \right] \tag{6}$$

The pressure ratio is obtained from a simulation of the expansion 4-5 accounting for ice formation. The transformation is reconstructed as a series of equilibrium states, iteratively calculating the inlet condition that gives the required outlet temperature after a “humid expansion” process, which accounts for the possible phase-change of the vapour. Pressure losses in the heat exchangers being neglected, compression ratio and expansion ratio are equal. The adopted method for the calculation of π accounts for the deviation of the real expansion process from the ideal adiabatic-isentropic transformation of the humid air by means of the expansion efficiency defined in eq. (7).

$$\eta_T = \frac{J_4 - J_5}{J_4 - J_{5is}} \tag{7}$$

where point 5_{is} is defined with reference to the thermodynamic state at turbine inlet ($s_{5is}=s_4$). Enthalpy and entropy of the humid air are calculated as follows:

$$J = h_{air} + x_4 h_v \tag{8}$$

$$s = s_{air} + x_4 s_v \tag{9}$$

where x is the absolute humidity of the working air stream. Water enthalpy and entropy are evaluated assuming ideal gas behaviour until saturation, whereas after saturation they are given, respectively, by eq.s 10 and 11.

$$h_v = h_{v,sat} - \left(1 - \frac{x_5}{x_4}\right) r \tag{10}$$

$$s_v = s_{v,sat} - \left(1 - \frac{x_5}{x_4}\right) \frac{r}{T} \tag{11}$$

r being the latent heat of ice formation. When phase change occurs, the total flowrate includes the three contributions of ice, vapour and dry air flowrates. If the absolute humidity decreases with respect to the preceding step, the difference is taken as the quantity of ice produced. The ice formation is considered as instantaneously defined by eq. 12; where the vapour and the ice flowrates change with the local temperature, whereas the dry air's flowrate stays constant.

$$\dot{m}_{ice} = \left(x_4 - x_{sat}\right) \dot{m}_{air} \tag{12}$$

The corresponding latent heat release is added to the air enthalpy (eq. 13);

$$J = \frac{\dot{m}_{air} h_{air} + \dot{m}_v h_{v,sat} + \dot{m}_{ice} r}{\dot{m}_{air}} \tag{13}$$

and a corrected temperature is calculated via NIST functions. Pressure P_4 is calculated by iteratively increasing its value, from an initial one that gives the due state (state 5) at the end of an isentropic expansion, until the eq. 7 is verified with a preset tolerance.

Once the compression ratio is known, all properties can be calculated throughout the cycle. The amount of ice collected is define by eq. 12 and the cooling capacity is

$$Q_{f-RS} = \dot{m}_{air} \left(J_6 - J_5\right) \tag{14}$$

2.2 Heat Transfer surfaces

The cascade system presented eliminates the low temperature heat transfer surface, but features an air-refrigerant heat exchanger between the top and bottom cycles, and introduces an air-air regenerator, which might suffer from high pressure drops. A good design requires a compromise between volume of the heat

exchanger and related pressure drops. Considering the definition from Kays and London [29], the evaporator has effectiveness,

$$\varepsilon_{eva} = \frac{Q_{eva}}{Q_{\max}} = \frac{Q_{eva}}{C_{\min}\left(T_2 - T_{10}\right)} = \left(1 + \frac{\Delta T_{eva,\min}}{T_2 - T_{LD}}\right)^{-1} \tag{15}$$

where, due to the refrigerant phase-change occurring on the vapour compression cycle side, the minimum thermal capacity C_{min} pertains to the air flux circulating in the inverse Brayton cycle. Referring to eq.s 4-6,

$$\varepsilon_{eva} = \left(1 + \frac{\Delta T_{eva}}{\left[T_{RS} + \varepsilon_R\left(T_{LD} - T_{RS}\right)\right]\left\{1 + \frac{1}{\eta_C}\left[\frac{\left(1-\varepsilon_R\right)\left(T_{LD} - T_{RS}\right) + \Delta T_{5-6}}{\left(T_{RS} - \Delta T_{5-6}\right)\eta_T}\right]\right\} - T_{LD}} \right)^{-1} \tag{16}$$

Equation (16) highlights the dependence of the effectiveness of the cascade heat exchanger (evaporator of the top cycle) on the effectiveness of the regenerative heat exchanger of the Brayton cycle. Introducing the general expression of the effectiveness of a counter-current flow heat exchanger as a function of the number of transfer unit $NTU=\beta S/C_{min}$,

$$\varepsilon = \frac{1 - e^{-NTU\left(1 - C_{\min}/C_{\max}\right)}}{1 - \frac{C_{\min}}{C_{\max}} e^{-NTU\left(1 - C_{\min}/C_{\max}\right)}} \tag{17}$$

the total transfer surface required by the low temperature cycle may be written as a function of the regenerator effectiveness (Fig. 7). Specifically, C_{min} / C_{max} being 0 for the cascade Heat exchanger and 1 for the regenerative heat exchanger, equation (17) yields:

$$\varepsilon_R = \frac{NTU}{1 + NTU} \quad , \quad \varepsilon_{eva} = 1 - e^{-NTU} \tag{18}$$

A higher regenerator effectiveness ε_R reduces the load at the cascade heat exchangers $\dot{m}_{air}\, c_p(T_2\text{-}T_3)$ for the same air flowrate and, consequently, the size of the heat exchanger (Fig. 7) required to achieve a target minimum temperature difference $\Delta T_{eva,min}$.

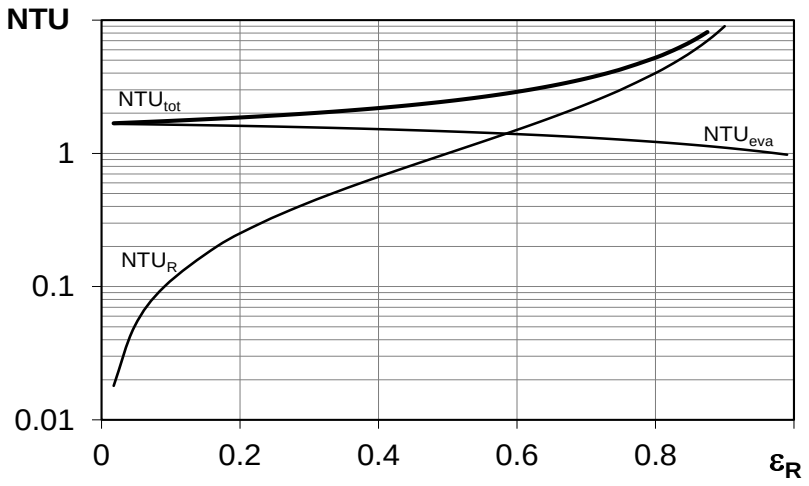

316

317 Figure 7. *NTU*-ε_R diagram of the bottom cycle

318

319 A higher regenerator effectiveness reduces also the compression ratio required for a given operative
320 temperature difference T_{LD}-T_{RS}, therefore increasing cycle efficiency.

321 In the regenerator, the hot and cold flows have practically equal thermal capacities and the driving
322 temperature difference is approximately constant along the axial length of the heat exchanger *L* (eq. 19).

323 $$Q_R = \dot{m}_{air} c_p \left(T_{LD} - T_4\right) = \dot{m}_{air} c_p \varepsilon_R \left(T_{LD} - T_{RS}\right) = \int_0^L \beta\eta\alpha A \Delta T dl = \beta\eta\alpha A \Delta T L \tag{19}$$

324 where β is the convective heat transfer coefficient, α the value of transfer area per unit volume, η is
325 the global effectiveness of the exchange surface and *A* is the frontal flow area. Neglecting the wall thermal
326 resistance, the solid surface temperature T_p corresponds to the mean value between the two streams,

327 $$\left|T - T_p\right| = \frac{\varepsilon_R \left(T_{LD} - T_{RS}\right)}{2} = \Delta T \tag{20}$$

328 Accordingly, by introducing the mass velocity of the air flow G_{air} circulating in the low temperature
329 cycle,

330 $$\varepsilon_R = \frac{\beta\eta\alpha L}{2G_{air} c_p + \beta\eta\alpha L} \tag{21}$$

331 The heat transfer coefficient β refers to the experimental correlation of Colburn factor reported by
332 Kays and London [29] and η is assumed to be 0.77 for realistic values of convective heat transfer coefficient

and usual fin geometry. The same reference gives the calculation procedure for the global pressure losses (inlet boundary-layer-separation drop, distributed losses through the passages and outlet recovery)

Table 3 - Possible features of a counter-flow regenerator with $\varepsilon = 0.9$.

Transfer surface per unit volume (m^{-1})	α	899
Regeneration effectiveness	ε_R	0.9
Global effectiveness of the exchange surface	η	0.77

Case 1			**Case 2**		
Mass velocity ($kg \cdot m^{-2} s^{-1}$)	G_{air}	13.7	Mass velocity ($kg \cdot m^{-2} s^{-1}$)	G_{air}	6.37
Pressure drops hot side (kPa)	ΔP	2.59	Pressure drops hot side (kPa)	ΔP	0.64
Pressure drops cold side (kPa)	ΔP	4.15	Pressure drops cold side (kPa)	ΔP	1.02
Axial length (m)	L	2.00	Axial length (m)	L	1.20
Frontal area (m^2)	A	0.95	Frontal area (m^2)	A	2.04

The regenerator features are listed in Table 3, for a target effectiveness of 0.9. This tentative sizing of the regenerator supports the feasibility of the selected design parameters shown in Table 1, where the assumed efficiency ε_R is conservative if compared to the claimed value (ε_R~95%) of the counter-flow regenerator featured by the 30 kW commercial product "Pascal Air" operating at design condition (NEDO documents [28]).

Case 1 features a smaller frontal cross-section area (higher mass velocity) and overall volume, but has higher pressure drop. Case 2 has a length L=1.2 m and the volume increases, but the pressure drop is reduced significantly (ΔP=1.02 kPa). Therefore, the pressure drops of the regenerative heat exchanger are preliminarily considered to be negligible when compared to the overall pressure ratio π of the bottom cycle and disregarded with respect to the whole system performance.

3. RESULTS AND DISCUSSION

As a first step, we consider the cascade system serving the refrigerated space *RS* without any additional cooling load due to the loading dock. In this case, as all the cooling power is delivered at the

minimum temperature, the system operates in its most severe condition. Assuming the reference parameter values listed in Table 2, the system performance is summarized in Table 4.

In this configuration the compression ratio turns out to be π=1.26, yielding a very low temperature rise within the compressor (T_1=1.5°C; T_2=23.6°C). With respect to state-of-the-art centrifugal compressors used for refrigeration, π is lower by one order of magnitude. This means that the turbine and compressor may have a very simple design and fairly high efficiency, e.g. they may both have a single axial stage. Furthermore, this temperature increase copes well with the superheating at the exit of the cascade heat exchanger (evaporator E_2 in Fig. 2), yielding acceptable heat transfer irreversibility.

Table 4 - Performance parameters with 100% cooling capacity given to *RS*.

Brayton cycle mass flow rate (kg·s^{-1})	$\dot{m}_{air}$	5.49
Cooling capacity (kW)	$Q_{f\text{-}RS}$	57.6
Power consumption, vapour compression cycle (kW)	W_{VC}	26.5
Power consumption, Brayton cycle (kW)	W_B	50.1
Coefficient Of Performance	COP	0.75
Water vapour subtracted (kg·h^{-1})	$\dot{m}_{H_2O}$	3.06

Note also the amount of vapour subtracted to the *RS*, which highlights the significant de-humidification potential of this system. Obviously the details of the ice-capturing device are outside the scope of this paper and must be tailored on the quantity and quality (particle dimension, density, etc.) of the removed ice by a careful experimental analysis.

The COP value shown in Table 4 may be compared with the data listed in Table 1 and Fig. 1. However, these values should be decreased to account for internal loads related to evaporator fans and defrosting. According to ASHRAE Refrigeration Handbook [24], these contributions may amount to 15% of the total cooling load. This power penalty enters in the COP calculation both as a reduction of cooling capacity and as an increase of energy consumption. Another term of comparison can be a stand-alone

Brayton cycle covering all the temperature range between ambient and refrigerated space. In this case the COP would fall to 0.55.

As the cooling power delivered to the loading dock increases, the cascade system shows a relentless performance improvement, up to a COP of 1.4 when half of the cooling capacity from the top cycle is delivered at the temperature level of the LD. Obviously the aforementioned results are strictly dependent on the parameters chosen for the simulation.

3.1 – Effect of compressor and turbine efficiency

If the compressor and/or turbine efficiency are improved or decreased, the system COP is heavily influenced, as shown in Fig. 8 for Q_{LD}/Q_{VC} = 0.25. In general, for given cold store and loading dock temperatures, higher expander and compressor efficiency are associated to lower required pressure ratios. The analytic expression of the dependence of the COP of the Brayton cycle on the polytropic efficiency of the turbine and the compressor has been described by Giannetti and Milazzo in [18].

The inclined surface drawn in Fig. 8 is practically symmetric, i.e. the effect of improving the compressor or the turbine is equally important. This result could change if the effect of pressure losses through heat exchangers, piping and ice filter were included in the analysis. A further pressure reduction may be due to the need to introduce the air within the *RS* at a suitable speed in order to promote circulation.

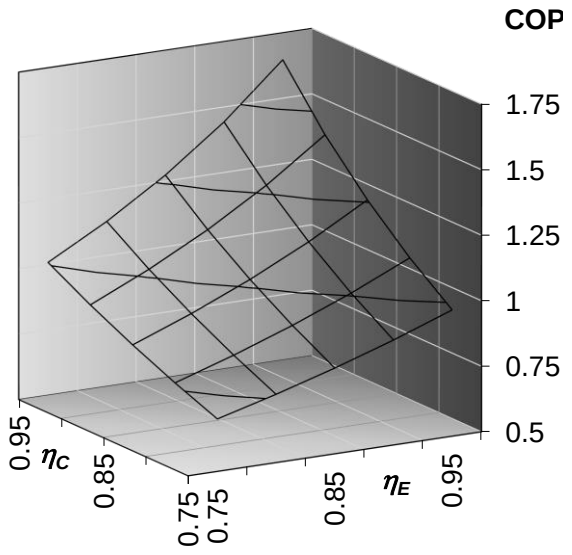

Figure 8. Cascade system COP v/s compressor and turbine efficiencies (Q_{LD}/Q_{VC} = 0.25)

3.2 Effect of Regenerator effectiveness

The regenerator effectiveness ε_R also has a significantly beneficial influence, especially at high values, as shown in Fig. 9 for the same value of Q_{LD}/Q_{VC}. Ceteris paribus, a higher ε_R reduces the gap between the source temperature and the inlet temperature to the turbine or compressor, lowering the compression ratio π required for a specific application case.

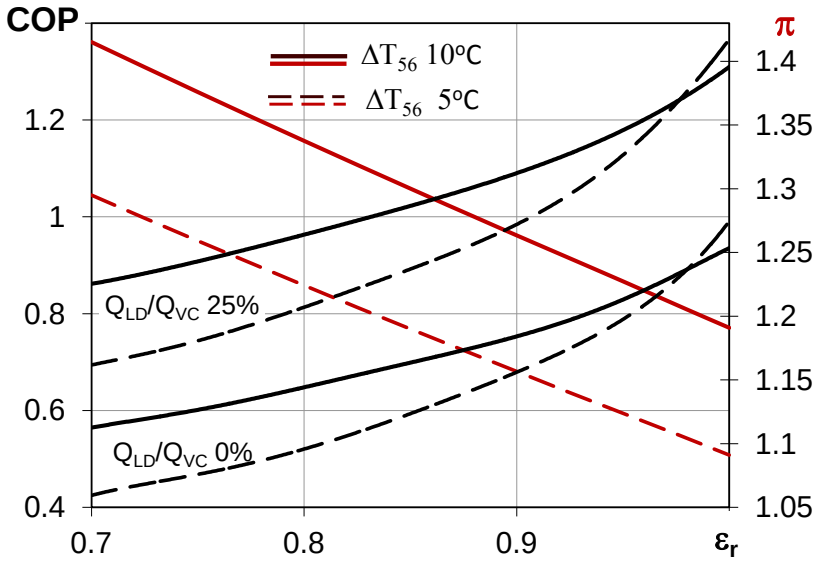

Figure 9. Cascade system COP v/s regenerator effectiveness

Increasing the regenerator surface is probably the simplest way to improve the air cycle performance, though a great care must be taken to avoid a corresponding increase in pressure loss [18]. The high reference value assumed for effectiveness has been proven to be feasible in terms of heat exchange surface by the conceptual design reported in the previous section. The same can be said of evaporators and condenser, where rather low temperature differences have been imposed.

3.3 Effect of cold air inlet temperature

Another significant parameter is the temperature difference between refrigerated space and air inlet ($\Delta T_{5\text{-}6}$). Figure 10 shows how a reduction of this temperature difference yields a corresponding decrease of π.

A higher regenerator effectiveness better matches lower $\Delta T_{5\text{-}6}$ and, conversely, lower values of the latter parameter turn out to be beneficial when a highly efficient regenerator is not available. The effect of $\Delta T_{5\text{-}6}$ on the system COP is also visible in Fig. 10, which shows a well-defined maximum for each value of Q_{LD}/Q_{VC}. Specifically, the value of $\Delta T_{5\text{-}6}$ yielding the maximum performance increases as the regenerator effectiveness is reduced. The same behaviour was also shown in terms of air flow rate or specific cooling capacity in [18].

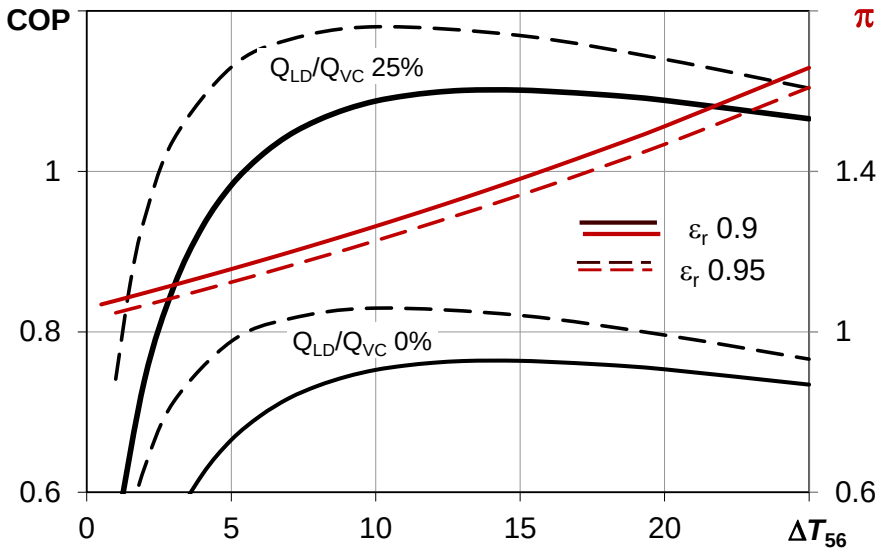

Figure 10. Cascade system COP v/s $\Delta T_{5\text{-}6}$

Every refrigeration system faces finite capacity heat sources that can be approximated to isothermal sources with different degrees of approximation. However, some applications, counter current products refrigeration on contact belt freezers for instance, require large temperature variations of the low temperature heat source. In these cases, if the system is designed to deliver the refrigerant in counter-current to the belt movement, a higher $\Delta T_{5\text{-}6}$ could indeed minimize heat transfer irreversibility and lead to higher overall system efficiency.

As the temperature difference increases (i.e. the air flow decreases), so does the difference in absolute humidity between inlet flow and *RS* air, enhancing the drying capability of the system. On the other hand, a lower flowrate directly implies a lower rate of humid air processed within the Brayton cycle. Figure 11 highlights a maximum of the humidity removal rate (i.e. amount of ice formed per unit time) at a specific

value of $\Delta T_{5\text{-}6}$. If the cold-store temperature decreases from -30 to -50, the maximum removal rate moves to the right.

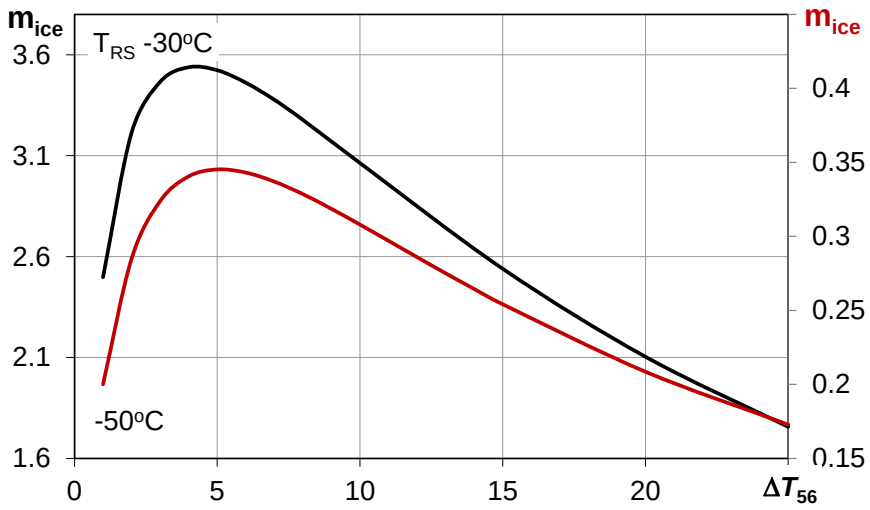

Figure 11. Rate of humidity extracted for different cold-store temperatures

3.4 Effect of inter-cooled compression

As already mentioned, the efficiency gap of the Brayton cycle decreases at lower cold space temperatures. Therefore, further calculations have been made for values below -30°C. In this case, an inter-cooled compression could be advantageous in order to keep the compression ratio and compressor exit temperature at low values (Fig. 13). A possible scheme is shown in Fig. 12.

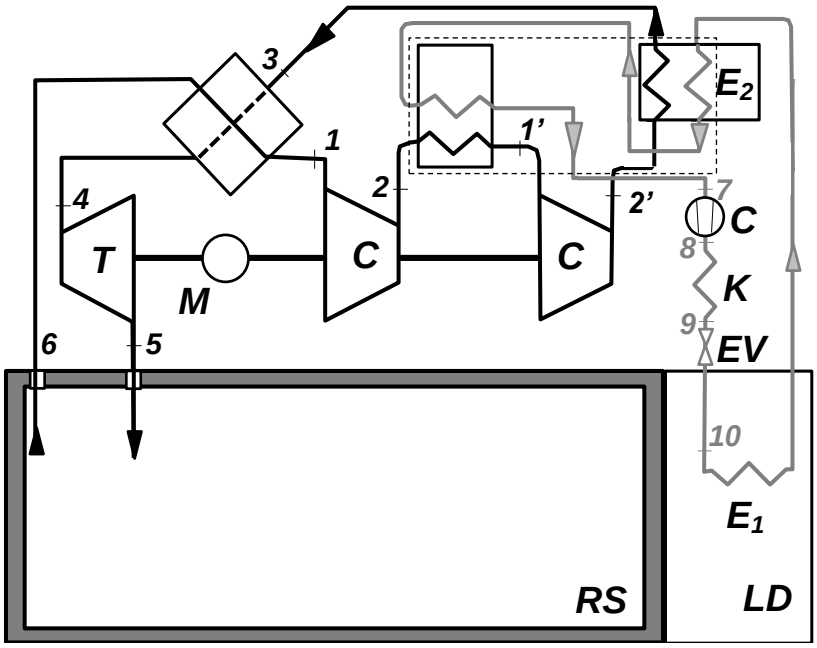

Figure 12. Scheme of the cascade system featuring inter-cooled staged compression on the Brayton cycle

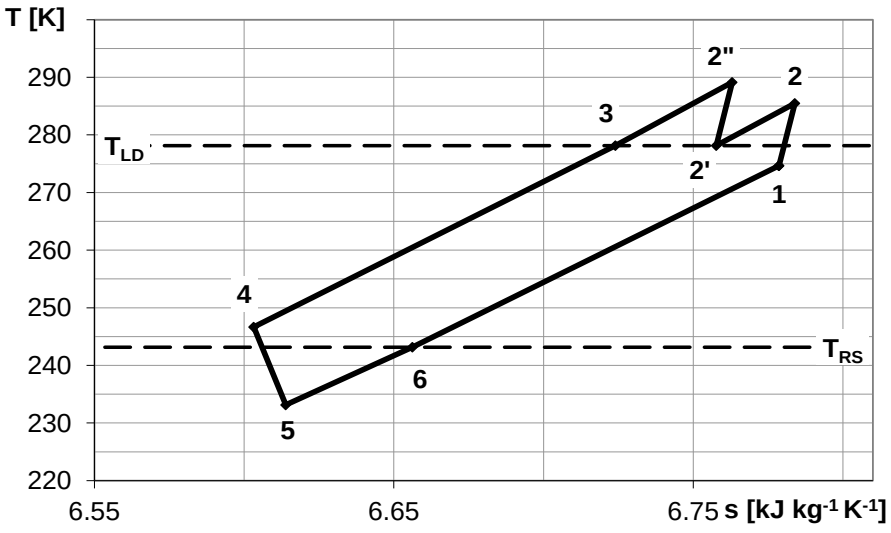

Figure 13. Temperature-entropy diagram for Brayton cycle with inter-cooled compression ($\Delta T_{5\text{-}6}=7^{o}C$)

When compared with single stage compression, the intercooled configuration copes with higher temperature variation at the cold storage, i.e. lower air flowrates. As shown in Fig.14 the COP gain is not dramatic, but may become worth the effort at high values of $\Delta T_{5\text{-}6}$.

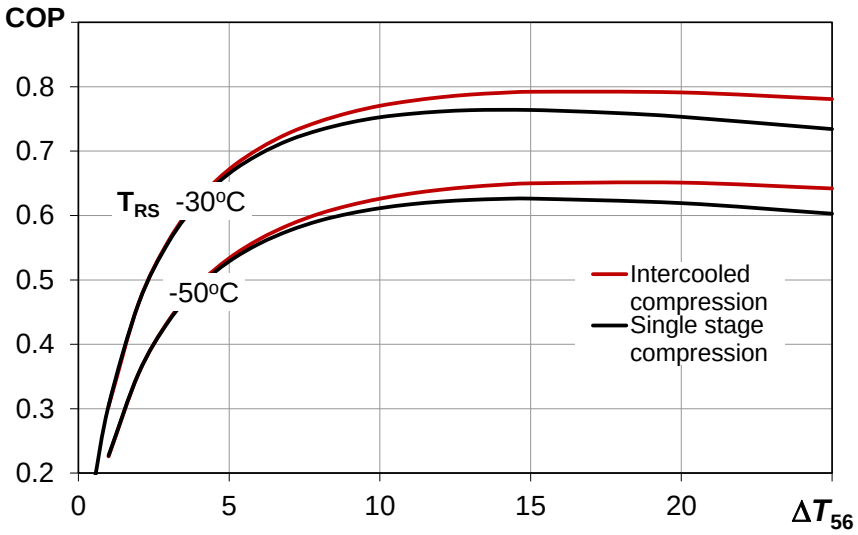

452

453 Figure 14. COP as a function of $\Delta T_{5\text{-}6}$ for various cold space temperatures, with (grey lines) and without

454 (black lines) intercooling (Q_{LD}/Q_{VC} = 0%)

455

456 3.5 Effect of cold space temperature

457 When the cold space temperature is used as a parameter, the comparison between conventional

458 systems (Table 1, Fig. 1) and the one presented here (continuous lines in Figure 15) becomes clearer:

459 accounting for COP losses due to defrosting and cold air circulation of the conventional systems the

460 performance of the cascade Brayton system becomes competitive at low storage temperatures. A pure

461 Brayton cycle is shown for comparison (dashed line in Fig. 15).

462 Systems requiring very low temperature, e.g. fast freezing of food, may represent a promising

463 application for the proposed scheme. Air, in this case, may be the sole option, as shown e.g. by the

464 experiments performed at – 124.5°C by Hongli et al. [30].

465

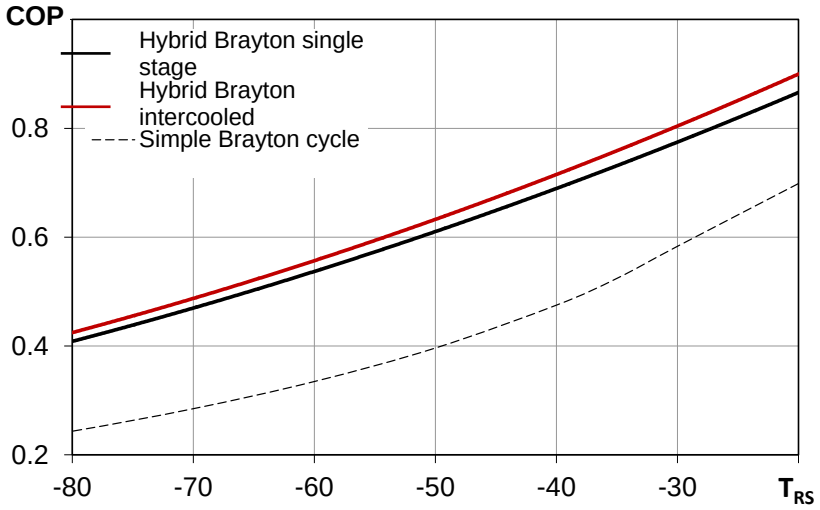

Figure 15. COP as a function of T_{RS} for various system configurations

4. CONCLUSIONS

A zero-GWP cascade configuration featuring an ammonia vapour compression cycle at the top and an inverse Brayton cycle at the bottom is proposed for cold store applications. The use of air as a working fluid in the bottom cycle eliminates the evaporator and the related thermal loads due to defrosting, as well as to the fan for air circulation. In a cascade configuration the regenerated Brayton cycle is characterized by a very low compression ratio, hence enabling the use of simple and highly efficient turbine and compressor. At the same time, this condition yields a lower temperature rise within the compressor and reduces the thermal irreversibility in the cascade heat exchanger.

The top cycle may also serve for loading dock refrigeration. The penalty in terms of COP can be low or even null, as soon as efficient compressor, turbine and regenerator are available. This target is becoming technically feasible as design and manufacturing of turbomachinery and heat exchangers progress. Additionally, as the operating temperature is lowered the efficiency gap with respect to conventional systems decreases or even vanishes, while other fluids (e.g. CO_2) reach their triple point and become unusable.

An optimum value exists for the temperature difference between cold air admission and refrigerated space. Latent load may be handled by an ice capturing device installed at the turbine outlet port.

If the refrigerated space temperature is very low, a staged-intercooled compression may offer a further slight increase in efficiency.

The proposed configuration seems promising in terms of safety (low pressure, ammonia used only outside of the cold space), reliability (no need to defrost, no electric fan in the cold space) and environment protection (both cycles use “natural” fluids). The system turns out to be readily feasible, given the well-established background of each of the two integrated refrigeration technologies.

As long as the loading dock temperature is moderate (e.g. 5°C as assumed herein), this concept can be extended by coupling the Brayton cycle with a heat driven refrigeration system, i.e. an absorption or ejector chiller, in lieu of the electric-driven ammonia cycle. In this way, the electric energy consumed by the Brayton cycle and the thermal energy for the heat driven chiller could be both produced by a combined heat and power system (CHP), allowing significant energy savings.

ACKNOWLEDGMENT

This work has been supported by MIUR of Italy within the framework of PRIN2015 project «Clean Heating and Cooling Technologies for an Energy Efficient Smart Grid»

REFERENCES

[1] Bingming, W., Huagen, W., Jianfeng, L., Ziwen, X. 2009, Experimental investigation on the performance of NH_3/CO_2 cascade refrigeration system with twin-screw compressor, *Int. J. Refrig.* 32: 1358-1365.

[2] Kilicarslan A., Hosoz M. 2010, Energy and irreversibility analysis of a cascade refrigeration system for various refrigerant couples: *Energy Conversion and Management* 51 (12): 2947-2954.

[3] Lee, T.S., Liu, C.H., and Chen, T.W. 2006, Thermodynamic analysis of optimal condensing temperature of cascade-condenser in CO_2/NH_3 cascade refrigeration systems, *Int. J. Refrig.* 29: 1100-1108.

[4] Di Nicola. G., Giuliani, G., Polonara, F., Stryjek, R., Arteconi, A. 2011, Performance of cascade cycles working with blends of CO_2 + natural refrigerants, *Int. J. Refrig.* 34: 1436-1445.

[5] Aminyavari M., Najafi B., Shirazi A., Rinaldi F. 2014, Exergetic, economic and environmental (3E) analyses, and multi-objective optimization of a CO2/NH3 cascade refrigeration system, *Applied Thermal Eng.* 65 (1–2): 42-50.

[6] Nasruddin, Sholahudin S., Giannetti N., Arnas 2016, Optimization of a cascade refrigeration system using refrigerant C3H8 in high temperature circuits (HTC) and a mixture of C2H6/CO2 in low temperature circuits (LTC), *Applied Thermal Eng*. 104: 96-103.

[7] Gettu. H.M, Bansal. P.K. 2008, Thermodynamic analysis of an R744-R717 cascade refrigeration system, *Int. J. Refrig.* 31: 45-54.

[8] Mosaffa A.H., Garousi Farshi L., Infante Ferreira C.A., Rosen M.A. 2016, Exergoeconomic and environmental analyses of CO2/NH3 cascade refrigeration systems equipped with different types of flash tank intercoolers, *Energy Conversion and Management* 117: 442-453.

[9] Dopazo, J.A., Fernandez-Seara J. 2011, Experimental evaluation of a cascade refrigeration system prototype with CO_2 and NH_3 for freezing process applications, *Int. J. Refrig.* 34 (1): 257-267.

[10] Sanz-Kock C., Llopis R., Sánchez D., Cabello R., Torrella E. 2014, Experimental evaluation of a R134a/CO2 cascade refrigeration plant, *Applied Thermal Eng.* 73 (1): 41-50.

[11] www.ammonia21.com

[12] Zhang Y., Chen J., He J., Wu C. 2007, Comparison on the optimum performance of the irreversible Brayton refrigeration cycles with regeneration and non-regeneration, *Applied Thermal Eng.* 27: 401-407.

[13] Chen L., Tu Y., Sun F. 2011, Exergetic efficiency optimization for real regenerated air refrigerators, *Applied Thermal Eng.* 31: 3161-3167.

[14] Ust Y. 2009, Performance analysis and optimization of irreversible air refrigeration cycles based on ecological coefficient of performance criterion, *Applied Thermal Eng.* 29: 47-55.

[15] Yannopoulos S.I., Lyberatos G., Theodossiou N., Li W., Valipour M., Tamburrino A., Angelakis A.N., Evolution of Water Lifting Devices (Pumps) over the Centuries Worldwide, Water 2015, 7(9), 5031-5060.

[16] Gladstone J., John Gorrie the visionary, ASHRAE Journal, December 1998.

[17] Grazzini G, Milazzo A. 2010, Air cycle air conditioning: analysis of different configurations, *Proc. Sustainable Refrigeration and Heat Pump Technology Conference*: *1-8*.

[18] Giannetti N, Milazzo A. 2014, Thermodynamic analysis of regenerated air-cycle refrigeration in high and low pressure configuration, *Int. J. Refrig.* 40: 97-110.

[19] Nóbrega C.E.L, Sphaier L.A. 2012, Modelling and simulation of a Desiccant-Brayton Cascade refrigeration cycle, *Energy and Buildings*, 55: 575-584.

[20] Elsayed S.S., Miyazaki T., Hamamoto Y., Akisawa A., Kashiwagi T. 2008, Performance analysis of air cycle refrigerator integrated desiccant system for cooling and dehumidifying warehouse, *Int. J. Refrig*, 31 (2): 189-196.

[21] Boone J., Machida A. 2011, Development of air refrigeration system "Pascal Air". *Proc. 23rd Int. Congr. Refrig*., IIF/IIR: 1597-1605.

548 [22] Kikuchi S, Igawa H, Mitsuhashi M, Okuda S, Morii S, Higashimori H. 2005, Development of air cycle
549 system for refrigeration. *Mitsubishi Heavy Ind. Tech. Rev*. 42: 1-4.
550 [23] Gigiel A, Giuliani G, Vitale C, Polonara F. 2006. An open air cycle freezer. *Proc. 7th Gustav*
551 *Lorentzen Conf. Nat.Work. Fluids*, IIF/IIR: 325-328.
552 [24] ASHRAE. 2010, *Handbook - Refrigeration*, American Society of Heating, Refrigeration and Air-
553 Conditioning Engineers, inc. Atlanta, GA.
554 [25] https://www.bitzer.de/websoftware/Calculate.aspx
555 [26] Lemmon E.W., Huber M.L., McLinden M.O. 2013, *NIST Standard Reference Database 23: Reference*
556 *Fluid Thermodynamic and Transport Properties-REFPROP, Version 9.1*. National Institute of
557 Standards and Technology, Standard Reference Data Program, Gaithersburg, Maryland, USA.
558 [27] ASHRAE. 2009, *Handbook - Fundamentals*, American Society of Heating, Refrigeration and Air-
559 Conditioning Engineers, inc. Atlanta, GA.
560 [28] NEDO PROJECT SUCCESS STORIES November 2013, *Documents,エネルギー問題解決に挑む、*
561 *空気冷媒でマイナス 60 を実現する超低温冷凍システム (An ultra-low temperature refrigeration*
562 *system that realizes minus 60 with air refrigerant, challenging energy problem solution, Maekawa*
563 *Manufacturing co., Ltd.)、株式会社前川製作所 (Mayekawa Co. Ltd.), Japan (in Japanese)*.
564 [29] Kays W. M. and London A. L. 1964, Compact Heat Exchangers, 2nd edition, McGraw-Hill, New
565 York.
566 [30] Hongli Z., Yu H., Liang C. 2009, Experimental study on a small Brayton air refrigerator under -120
567 °C, Applied Thermal Eng. 29: 1702-1706.
568